

---

# Faaa: Sites M0019 and M0020<sup>1</sup>

---

Expedition 310 Scientists<sup>2</sup>

## Chapter contents

Operations . . . . .	1
Sedimentology and biological assemblages . . .	1
Petrophysics . . . . .	3
References . . . . .	5
Figures . . . . .	6

## Operations

### Hole M0019A

After arriving at Faaa from Hole M0018A (Maraa), the *DP Hunter* was positioned above Hole M0019A in 58 m water depth. All clearances with airport and seaport authorities were double checked before occupying the new location, which was closest to the visible reef so far. A seabed camera survey was run, and no live corals were observed. Seacore's drilling and reentry template (DART) was lowered and drilled in, and coring operations in Hole M0019A began at 2320 h on 4 November 2005. Coring was completed at 2400 h on 5 November at a total depth (TD) of 66.96 meters below seafloor (mbsf) and with a total recovery of 41.12%. Penetration was rapid, but recovery was poor. Checks of the Jean Lutz automatic drilling recorder data confirmed the driller's view that there were significant void spaces throughout. When the penetration rate reduced to below 10 m/h, indicating more solid material, core was usually obtained.

### Hole M0020A

Prior to coring in Hole M0020A, the DART was retrieved and a short echo sounder survey was conducted 50 m north of Hole M0019A to locate a site for Hole M0020A. The chosen site was checked using the tautwire, and the DART and drill pipe were deployed in 83 m water depth. Coring operations began in Hole M0020A at 1200 h on 6 November 2005 and continued until 1220 h on 7 November to a TD of 42.16 mbsf. Total recovery was 70.45%.

The *DP Hunter* departed the Faaa area at 1320 h on 7 November and proceeded to Site M0021 (Tiarei area).

## Sedimentology and biological assemblages

Sites M0019 and M0020 were drilled at 59.9 and 83.7 meters below sea level (mbsl), respectively. The boundary between the last deglacial and older Pleistocene sequences at the two sites, which is defined on the basis of lithological and diagenetic features, occurs at 82 and 92 mbsl in Holes M0019A and M0020A, respectively.

<sup>1</sup>Expedition 310 Scientists, 2007. Faaa: Sites M0019 and M0020. In Camoin, G.F., Iryu, Y., McInroy, D.B., and the Expedition 310 Scientists. *Proc. IODP*, 310: Washington, DC (Integrated Ocean Drilling Program Management International, Inc.). doi:10.2204/iodp.proc.310.110.2007

<sup>2</sup>Expedition 310 Scientists' addresses.



## Last deglacial sequence (Unit I)

Intervals: Cores 310-M0019A-1R through 10R-1 and 310-M0020A-1R through 7R

Lithologic Unit I recovered at Sites M0019 and M0020 is 21 and 8 m thick, respectively, and displays a very similar composition in the two holes.

The top of the sequence corresponds to a hardground and is characterized by extensive bioerosion and staining of the top 50 cm (Fig. F1) (e.g., interval 310-M0020A-1R-1, 3–9 cm). It is primarily composed of loose corallgal-microbialite frameworks (bindstone) interlayered with beds of coral rubble. The beds are composed of reworked and rounded fragments of coral colonies (branching agariciids and *Porites*), coralline algal crusts, and microbialites that are strongly bored and stained.

The corallgal-microbialite frameworks are dominated by encrusting colonies of *Montipora*, agariciids (*Pavona?*), *Acropora*, *Psammocora*, and *Echinophyllia* associated locally with massive colonies of *Porites*, *Montastrea*, and *Cyphastrea* and encrusting colonies of *Leptoseris* and by fragments of robust branching *Pocillopora*, tabular *Acropora*, and branching *Porites* in addition to the coral colonies listed above (Figs. F2, F3, F4, F5, F6) (e.g., intervals 310-M0019A-1R-1, 8–13 cm, 2R-1, 74–80 cm, 2R-1, 80–98 cm, and 9R-1, 72–86 cm, and 310-M0020A-2R-1, 57–64 cm, and 4R-1, 20–28 cm). The base of the last deglacial sequence is characterized by the occurrence of in situ robust branching colonies of *Pocillopora*, massive colonies of *Porites* (Cores 310-M0019A-9R and 10R), and tabular colonies of *Acropora* (Core 310-M0020A-7R); bioerosion is extensive in those intervals (Fig. F7) (e.g., interval 310-M0019A-9R-1, 32–38 cm).

Corals are usually coated with thin crusts of nongeniculate coralline algae. Microbialites consist of dark gray, laminated, dense, and thrombotic fabrics; the latter are usually dominant (Fig. F8) (e.g., interval 310-M0020A-4R-1, 0–10 cm). Large cavities, partly to fully filled with skeletal sand rich in *Halimeda* segments, commonly occur. Reddish brown to dark staining on the surface of reef rocks is conspicuous in Cores 310-M0019A-2R, 7R, and 8R and 310-M0020A-2R, 3R, 6R, and 7R. Corals display traces of alteration in Core 310-M0020A-5R.

## Older Pleistocene sequence (Unit II)

This sequence displays a distinctive composition in the two holes. The uppermost part of the older Pleistocene sequence (lithologic Unit II) is characterized by the occurrence of brown to dark staining.

### Hole M0019A

The older Pleistocene sequence recovered at Site M0019 is 43 m thick. This sequence includes three

subunits characterized by their distinctive lithology and composition and separated by unconformities at 106.2 (Core 310-M0019A-22R) and 121.12 (Core 310-M0019A-33R) mbsl, respectively.

### Subunit IIA

Interval: Section 310-M0019A-10R-1 through Core 22R

The upper subunit in Hole M0019A is 24 m thick and comprises irregular alternations of beige corallgal and skeletal limestone bearing in situ coral colonies and beds composed of coral rubble.

The coral assemblages forming the corallgal frameworks consist of massive colonies of *Porites* (e.g., Cores 310-M0019A-14R, 16R, and 18R through 20R), branching and encrusting colonies of *Porites*, and, to a lesser extent, encrusting colonies of *Porites*, agariciids, and *Montipora*, massive colonies of *Leptastrea* and *Montastrea*, and tabular colonies of *Acropora* (Figs. F9, F10, F11, F12, F13, F14) (e.g., intervals 310-M0019A-13R-1, 40–45 cm, 13R-1, 50–60 cm, 15R-1, 51–57 cm, 19R-1, 42–54 cm, 20R-1, 65–75 cm, and 22R-1, 35–50 cm). Fragments of branching *Pocillopora* occasionally occur. These coral colonies are generally thinly coated with nongeniculate coralline algae, locally associated with microbialite crusts, except in the lower part of the subunit, where coralline algal crusts are thicker and include vermetid gastropods.

Skeletal limestone consists of a well-lithified rudstone including subrounded fragments of coral colonies (massive and branching *Porites*, robust branching *Pocillopora*, and tabular *Acropora*) in many cases encrusted with nongeniculate coralline algae and locally surrounded by cement fringes. Other skeletal grains include *Halimeda* segments and fragments of echinoids, coralline algae, and mollusks. This limestone locally displays conspicuous alteration; walls of pores in many cases exhibit red-brown staining and in some cases are lined with yellow cements (Fig. F15) (e.g., interval 310-M0019A-10R-1, 70–85 cm).

Rubble beds are composed of fragments of coral colonies (branching and massive *Porites*, robust branching *Pocillopora*, and tabular *Acropora*) and are thinly encrusted with coralline algae and, locally, microbialites.

### Subunit IIB

Interval: Cores 310-M0019A-22R through 26R

Subunit IIB in Hole M0019A is 15 m thick and composed of yellowish brown skeletal floatstone to grainstone including rhodoliths, foraminifers, and fragments of corals (branching and encrusting *Porites*, robust branching *Pocillopora*, and tabular

*Acropora*) (Fig. F16) (e.g., interval 310-M0019A-22R-1, 50–70 cm) and coralline algae, echinoids, and mollusks; sand-sized volcanic grains occur in the lower part of this subunit, and their abundance increases downhole. Large coral fragments are usually thinly encrusted with coralline algae (Figs. F17, F18) (e.g., intervals 310-M0019A-22R-1, 102–108 cm, and 27R-1, 38–44 cm). In situ coral colonies (massive and encrusting *Porites* in Cores 310-M0019A-24R and 25R) occur locally.

### Subunit IIC

Interval: Cores 310-M0019A-27R through 34R

The lower subunit in Hole M0019A is 11 m thick and composed of irregular alternations of corallal frameworks, skeletal limestone, and rubble beds. Volcanic silt and sand and occasional volcanic gravels and pebbles occur as minor components in the carbonate units.

Corallal frameworks are dominated by tabular colonies of *Acropora*, massive colonies of *Porites* (e.g., Cores 310-M0019A-27R and 28R), encrusting colonies of *Porites* and *Montipora*, and robust branching colonies of *Acropora* (Figs. F19, F20) (e.g., intervals 310-M0019-27R-1, 68–83 cm, and 32R-1, 46–66). These coral colonies are heavily encrusted with nongeniculate coralline algae associated with vermetid gastropods. Sand-sized volcanic grains occur commonly in the matrix. Corals exhibit evidence of diagenetic alteration.

Skeletal rudstone is very poorly sorted and rich in large fragments of coral colonies (tabular *Acropora*, robust branching *Pocillopora*, branching *Porites*, and encrusting agariciids), rhodoliths, *Halimeda* segments, and fragments of coralline algae, mollusks, and echinoids (Figs. F21, F22, F23, F24) (e.g., intervals 310-M0019A-32R-1, 67–83 cm, 33R-2, 10–35 cm, 33R-2, 97–112 cm, and 33R-3, 82–104). Large fragments of corals are commonly encrusted with coralline algae. Sand- to pebble-sized volcanic grains are commonly present. Reddish to yellowish stains occur locally.

Rubble beds are composed of fragments of coral colonies (branching and massive *Porites*, robust branching *Pocillopora*, and tabular *Acropora*) thinly encrusted with coralline algae, rhodoliths, and basalt gravels and pebbles.

### Hole M0020A

Interval: Cores 310-M0020A-7R through 25R

In Hole M0020A, the sequence is primarily composed of corallal frameworks locally interlayered with skeletal limestone and rubble beds.

The corallal frameworks are dominated by massive, branching, and encrusting colonies of *Porites*, locally associated with encrusting colonies of *Montipora* and *Pavona*, and robust branching colonies of *Pocillopora* (Figs. F25, F26, F27, F28, F29, F30) (e.g., intervals 310-M0020A-10R-1, 40–47 cm, 12R-1, 65–80 cm, 16R-1, 56–70 cm, 18R-1, 49–58 cm, 20R-1, 89–101 cm, and 21R-2, 14–23 cm). These coral colonies are heavily encrusted with nongeniculate coralline algae associated with vermetid gastropods and serpulids and with microbialites (massive laminated fabrics overlain by thrombolitic accretions) (Figs. F31, F32, F33) (e.g., intervals 310-M0020A-12R-1, 34–50 cm, 18R-2, 0–15 cm, and 20R-1, 110–153 cm). Corals display traces of bioerosion and are locally strongly altered. Large vugs are partly filled with internal sediments and are commonly lined with cements. Walls of cavities and vugs display brown, red, to black staining throughout this interval. Large bioerosion cavities are locally filled with microbialite crusts (e.g., Core 310-M0020A-22R).

Massive *Porites* are dominant in several intervals (e.g., Cores 310-M0020A-14R, 15R, and 22R through 24R); a single colony of massive *Porites* ~3.5 m thick was recovered in Cores 310-M0020A-22R and 23R (Fig. F34) (e.g., interval 310-M0020A-22R-2, 16–29 cm).

Interlayered skeletal limestone consists of *Halimeda* wackestone and poorly sorted coral rudstone including fragments of branching and encrusting *Porites*, robust branching *Pocillopora* and *Acropora*, and encrusting *Montipora*. Other skeletal grains include *Halimeda* segments (Fig. F35) (e.g., interval 310-M0020A-25R-2, 0–17 cm) and fragments of mollusks and echinoids; volcanic silt to sand grains are locally abundant.

Rubble beds are comprised of fragments of coral colonies (branching *Porites*, *Pocillopora*, and *Pavona*).

## Petrophysics

Recovery at the two Faaa sites, on the northwestern side of the island of Tahiti, ranges from partial (Hole M0019A = 41%; Fig. F36) to good (Hole M0020A = 70%; Fig. F37). The two main units recovered at Faaa represent the last deglacial (lithologic Unit I) and older Pleistocene (lithologic Unit II) sequences. Cores 310-M0019A-23R, 24R, 26R, and 34R were left unsaturated and therefore have different data coverage and quality (see the “Methods” chapter for more details). Water depths are as follows: Hole M0019A = 58.75 mbsl; Hole M0020A = 83.30 mbsl.

## Density and porosity

Bulk density at Faaa sites was computed from gamma ray attenuation (GRA) using unsplit cores on the MSCL and from moisture and density (MAD) measurements on discrete plug samples. GRA bulk density measurements were near-continuous downcore for Hole M0020A (Fig. F37), and two intervals were recognized:

- Interval 1: 0–61 mbsf (Cores 310-M0019A-1R through 31R) and 0–36 mbsf (Cores 310-M0020A-1R through 23R): Data are scattered between 1.9 and 2.2 g/cm<sup>3</sup>.
- Interval 2: 61 mbsf to the bottom of the hole (Cores 310-M0019A-32R through 34R) and 36 mbsf to the bottom of the hole (Cores 310-M0020A-24R through 25R): The general bulk density trend is a gradual increase down to ~39 mbsf. Small-scale variations in density occur downhole between 39 and 42 mbsf; bulk density is rather uniform at ~2.6 g/cm<sup>3</sup>.

Density data for Hole M0019A (Fig. F36) from 20 mbsf to the bottom of the hole display high variability (note data gaps at 0–20, 30–40, 51, and 54 mbsf), and no distinct trends are identified in the upper sections. Below 61 mbsf, density shows a clear increase to values of ~2.4 g/cm<sup>3</sup>.

Grain density averages 2.74 g/cm<sup>3</sup> and shows no distinct pattern of variability as a function of depth. MAD density is between 1.95 and 2.43 g/cm<sup>3</sup> for the last deglacial sequence and increases to 2.60 g/cm<sup>3</sup> for the older Pleistocene sequence (e.g., 63 mbsf in Hole M0019A).

Values in Interval 2 are compatible with cementation and karstification below the Unit I/II boundary (see “[Sedimentology and biological assemblages](#)”), whereas Interval 1 has highly variable physical properties in the last deglacial sequence. Volcaniclastic input is common, resulting in higher densities (e.g., Hole M0019A from 61 mbsf down). With the exception of a few outliers, GRA bulk density values exceed MAD values by ~0.1 g/cm<sup>3</sup>.

Porosity profiles generally reflect a combination of stress history and sedimentological and diagenetic effects, such as variability in compressibility, permeability, sorting, grain fabric, and cementation. Porosity for MAD samples is calculated from the pore water content, assuming complete saturation of the wet sediment sample (see “[Moisture and density](#)” in the “[Methods](#)” chapter). The porosity curve from the MSCL mirrors the bulk density curve, as it is directly calculated from MSCL bulk density with a constant grain density of 2.71 g/cm<sup>3</sup> (see the “[Methods](#)” chapter). Porosity at Site M0020 varies between 20% and 55%. No distinct decrease of porosity with depth

is observed. No abrupt steps in porosity, a common characteristic of erosional unconformities, are observed within Unit I. A sharp decrease of porosity is observed at the transition in Interval 2 between 36 and 39 mbsf for Hole M0020A and 61 mbsf for Hole M0019A, which might indicate increased cementation. Cementation destroys porosity and increases density, one possible effect for diagenetic alteration attendant with subaerial exposure.

For Hole M0020A in Interval 2, low porosities with average values of ~15%–20% are the result of fine- to coarse-grained cemented skeletal limestone. MAD porosities all follow GRA porosities. Deviations (GRA) may occur because of the method of porosity calculation used, which cannot fully account for the multiminerall nature of the limestone with volcanoclastic influx.

## P-wave velocity

P-wave velocities were measured with the Geotek MSCL P-wave logger (PWL) on whole cores and the PWS3 contact sensor system on a modified Hamilton frame on ~2–4 cm long 1 inch round discrete samples of semilithified and lithified sediments (see the “[Methods](#)” chapter). Velocities in one transverse (x) direction were measured on the plugs. Extreme scatter and unreasonable velocities, likely a function of drilling disturbance, bad coupling, and lack of saturation, call into question the quality of the PWL, and data were therefore filtered for realistic values only. For Interval 1 in Hole M0019A, this results in scattered values and a highly discontinuous velocity profile. Only in Interval 2 is the record more continuous, with average velocities of up to 4700 m/s in Hole M0019A. Subsequent to filtering, Interval 1 consists of a group of relatively low velocities of ~1900 m/s and a group of higher velocities of ~3700 m/s (Fig. F36). Discrete measurements range from 3745 to 4782 m/s. For MAD properties, only samples sufficiently lithified and samples free of large pores were suitable for P-wave velocity measurements. As a result, mainly matrix sediments were sampled and the velocities from plug samples are generally located in the high spectrum of velocities. Values are all >3500 m/s and coincide with peaks in velocity measured with the PWL (Fig. F36). Hole M0020A shows a highly discontinuous and variable velocity profile, with the only distinct change in velocities occurring at ~61 mbsf (Interval 2) where velocity increases. Values of discrete measurements range from 3718 to 4705 m/s.

A cross plot of velocity versus porosity for Faaa sites shows a general inverse relationship (Fig. F38). For the time-average empirical equation of Wyllie et al. (1956) and Raymer et al. (1980), the traveltime of an

acoustic signal through rock is a specific sum of the traveltime through the solid matrix and the fluid phase. Porosity and velocity data show a poor match with the time-average equation and display large scatter around the general trend line. For a given density of 2.0 g/cm<sup>3</sup>, velocity may vary as much as 2000 m/s. No sonic logging data are available for Faaa sites.

### Magnetic susceptibility

Magnetic susceptibility values are a function of the mineralogy and concentration of magnetic minerals, with higher concentrations of ferromagnetic minerals such as magnetite, hematite, goethite, and titanomagnetite resulting in higher susceptibilities. The source of this material may be associated with influxes of volcanoclastic material. In the absence of ferromagnetic minerals, magnetic susceptibility displays low values induced by paramagnetic and diamagnetic minerals such as clay minerals and evaporites. Natural gamma radiation (NGR) values are a function of the terrigenous clay content within sediment. Clay minerals, being charged particles, tend to attract and bond with K, U, and Th atoms so that an increasing NGR count typically correlates with increasing clay/shale content. Both MS and NGR contain independent information concerning source provenance and magnetic mineral derivation. In clean carbonates, however, NGR is difficult to predict. Red algae are known to incorporate U, and as a result, intervals with dominant rhodoliths may show increased uranium response.

As described in “**Density and porosity**,” magnetic susceptibility measured at Faaa sites can be divided into two intervals with distinct patterns.

- In Interval 1, magnetic susceptibility is characterized by nearly constant amplitude from 0 to a maximum of  $50 \times 10^{-5}$  SI units.
- Interval 2 shows low recovery but generally low susceptibility except for a few outliers at ~3 mbsf (Hole M0019A). Interval 2 shows increased values ranging from 0 to  $250 \times 10^{-5}$  SI. It is inferred that Interval 2 represents times of enhanced terrigenous input in Pleistocene times, whereas the last deglacial sequence at the Faaa sites has very little volcanoclastic material admixed.

### Resistivity

See “**Resistivity**” in the “Maraa western transect” chapter.

### Diffuse color reflectance spectrophotometry

Color reflectance in the last deglacial sequence shows a variation of 38 to 86 L\* units (Fig. F39). Downhole trends are not present. High values of L\* (>70 L\* units) can be observed in the interval 32–35.4 mbsf (Sections 310-M0020A-22R-2 through 23R-2). These high values were measured on an interval of massive *Porites*. Lowest L\* values (40–61 L\* units) were measured on grainstone-dominated lithologies containing volcanoclastic grains. These lithologies are found at the base (53–55 mbsf) of the last deglacial sequence (Cores 310-M0019A-25R through 26R).

In the Cores 310-M0019A-33R through 34R (below 62.4 mbsf) within the older Pleistocene sequence, color reflectance has a relatively lower L\* value of 43–79 L\* units (average = 57 L\* units). This interval corresponds to rudstone with volcanoclastic grains (including basalt pebbles).

### Hole-to-hole correlation

Hole-to-hole correlation in carbonate reef environments is not an easy task. Heterogeneity in physical properties is large, and often only major unconformities can be identified. At Faaa, the best indication for correlation comes from magnetic susceptibility values together with abrupt changes in density, porosity, and velocity.

For example, Figure F37 shows an increase in magnetic susceptibility below 36 mbsf in Hole M0020A. In Hole M0019A, there is an increase in susceptibility at ~48 mbsf, although the exact change from low to high magnetic susceptibility probably occurs higher than this, within the poorly recovered section.

## References

- Raymer, L.L., Hunt, E.R., and Gardner, J.S., 1980. An improved sonic transit time-to-porosity transform. *Trans. SPWLA 21st Annu. Log. Symp.*, Pap. P.
- Wyllie, M.R.J., Gregory, A.R., and Gardner, L.W., 1956. Elastic wave velocities in heterogeneous and porous media. *Geophysics*, 21(1):41–70. doi:10.1190/1.1438217

**Publication:** 4 March 2007  
**MS 310-110**

**Figure F1.** Hardground (top of Unit I; interval 310-M0020A-1R-1, 3–11 cm). Volcanic grains are incorporated in thin coralline algal crusts. Note abundant borings in coral colonies and coralline algal crusts.

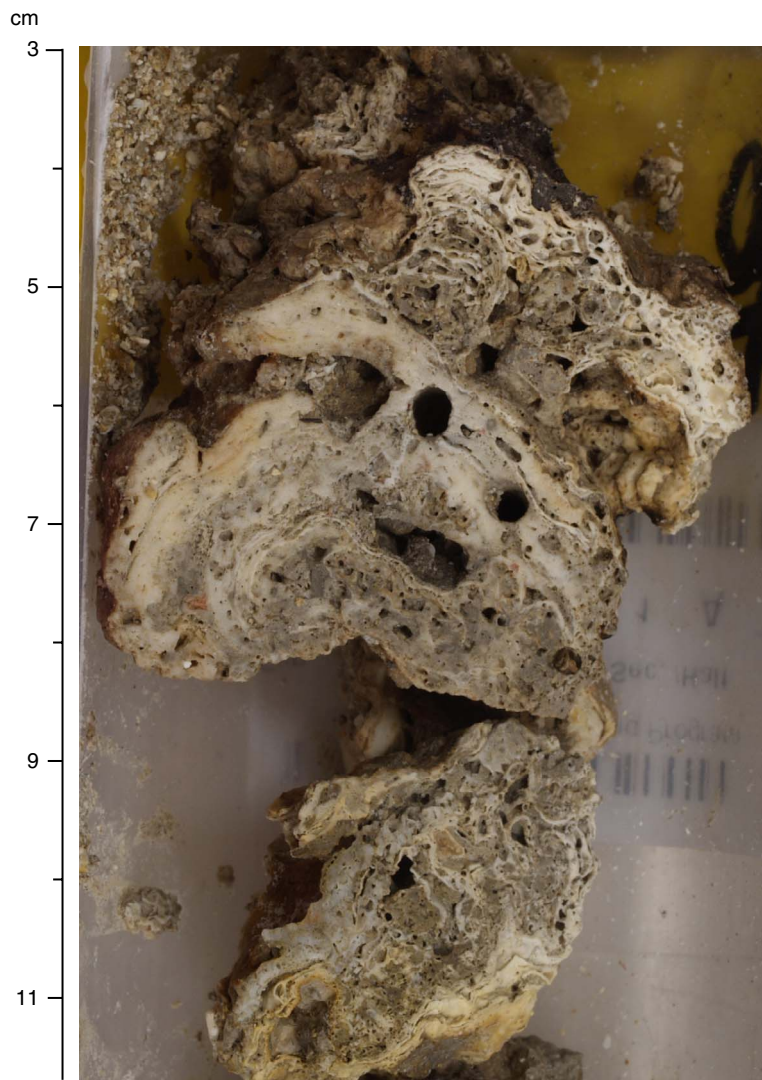


**Figure F2.** Tabular colony of *Acropora* with thin coralline algal crusts (Unit I; interval 310-M0019A-1R-1, 8–13 cm). Note extensive bioerosion of corals and coralline algae.



**Figure F3.** Encrusting colonies of agariciids (*Pavona*?) with multiple thin encrusting coralline algal crusts (Unit I; interval 310-M0019A-2R-1, 74–80 cm).

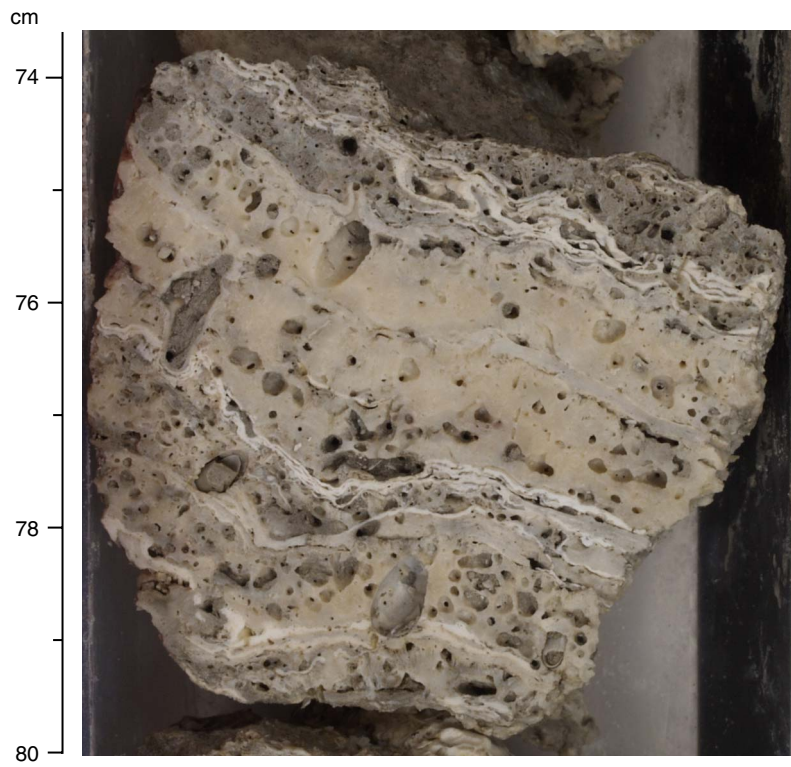


**Figure F4.** Massive colony of *Porites* (Unit I; interval 310-M0019A-2R-1, 80–98 cm). Lower part of figure shows encrusting coralline algae and microbialite masses.

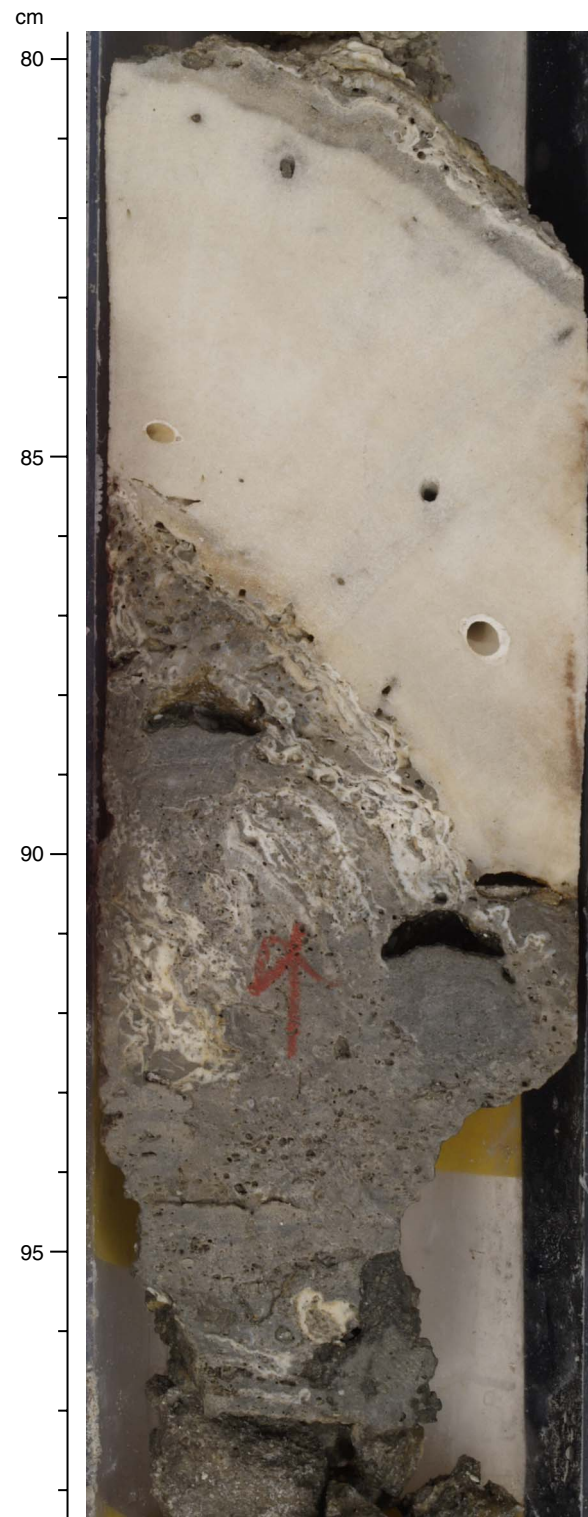


**Figure F5.** Encrusting colonies of agariciids and *Montastrea* encrusted with multiple thin coralline algal crusts and subsequent microbialites (Unit I; interval 310-M0019A-9R-1, 72–87 cm).



**Figure F6.** Encrusting colonies of *Montipora* and agariciids with coralline algal encrustations (Unit I; interval 310-M0020A-4R-1, 21–30 cm).



**Figure F7.** Extensive bioerosion in a robust branching *Pocillopora* colony covered with a coralline algal crust (Unit I; interval 310-M0019A-9R-1, 32–39 cm).

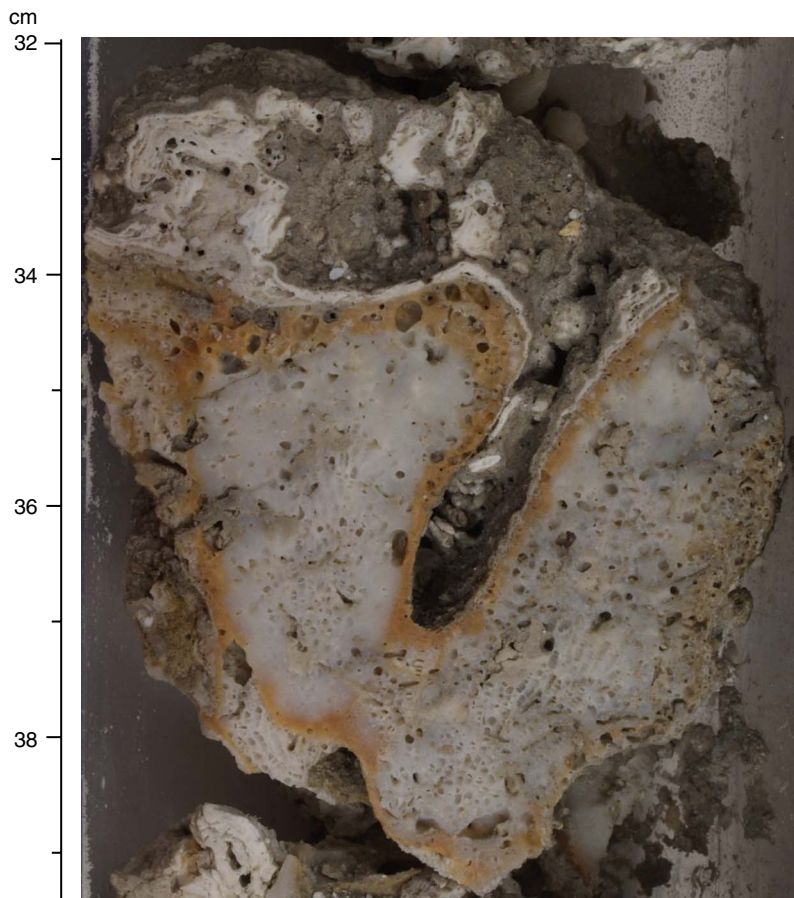
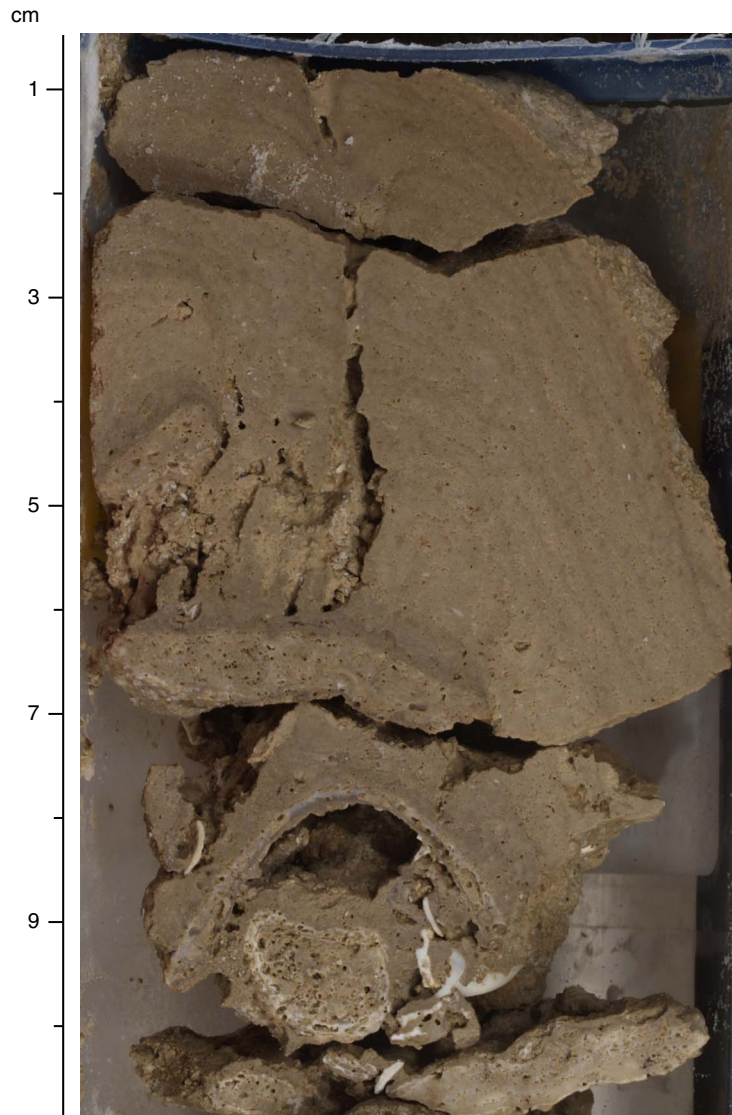


Figure F8. Massive laminated microbialite crust (Unit I; interval 310-M0020A-4R-1, 1–10 cm).



**Figure F9.** Branching and encrusting colonies of *Porites* with *Halimeda*-bearing sediment (Subunit IIA; interval 310-M0019A-13R-1, 41–46 cm).



**Figure F10.** Tabular *Acropora* colony encrusted with multiple thin coralline algal layers and vermetid gastropods (Subunit IIA; interval 310-M0019A-13R-1, 50–61 cm). Note bioerosion by bivalves.

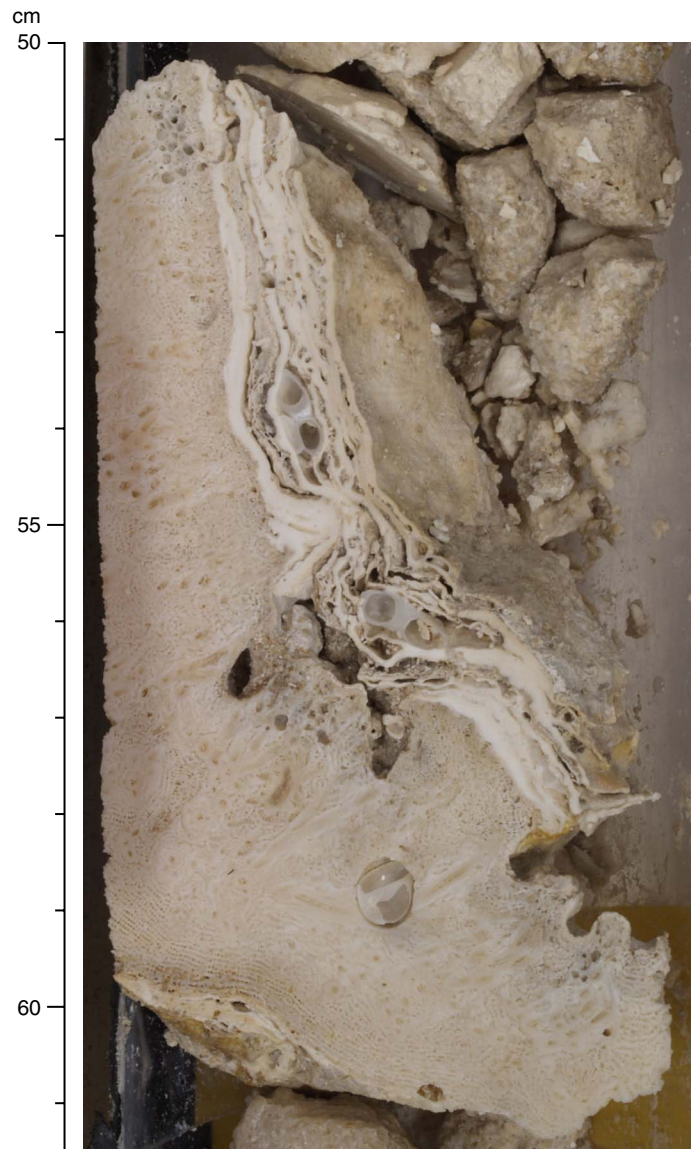


Figure F11. Massive colony of *Porites* (Subunit IIA; interval 310-M0019A-15R-1, 50–57 cm).



**Figure F12.** Massive *Montastrea* and encrusting *Porites* colonies interlayered with coralline algal crusts (Subunit IIA; interval 310-M0019A-19R-1, 43–54 cm). Note geopetal cement infill.



Figure F13. Encrusting colonies of *Porites* (Subunit IIA; interval 310-M0019A-20R-1, 64–75 cm).



**Figure F14.** Encrusting colonies of *Porites*, *Montipora*, and agariciids thinly encrusted with coralline algae (Sub-unit IIA; interval 310-M0019A-22R-1, 34–51 cm).



**Figure F15.** Skeletal rudstone with abundant massive and branching *Porites* fragments and *Halimeda* segments (Subunit IIA; interval 310-M0019A-10R-1, 69–89 cm). Note cement fringes around primary pores.

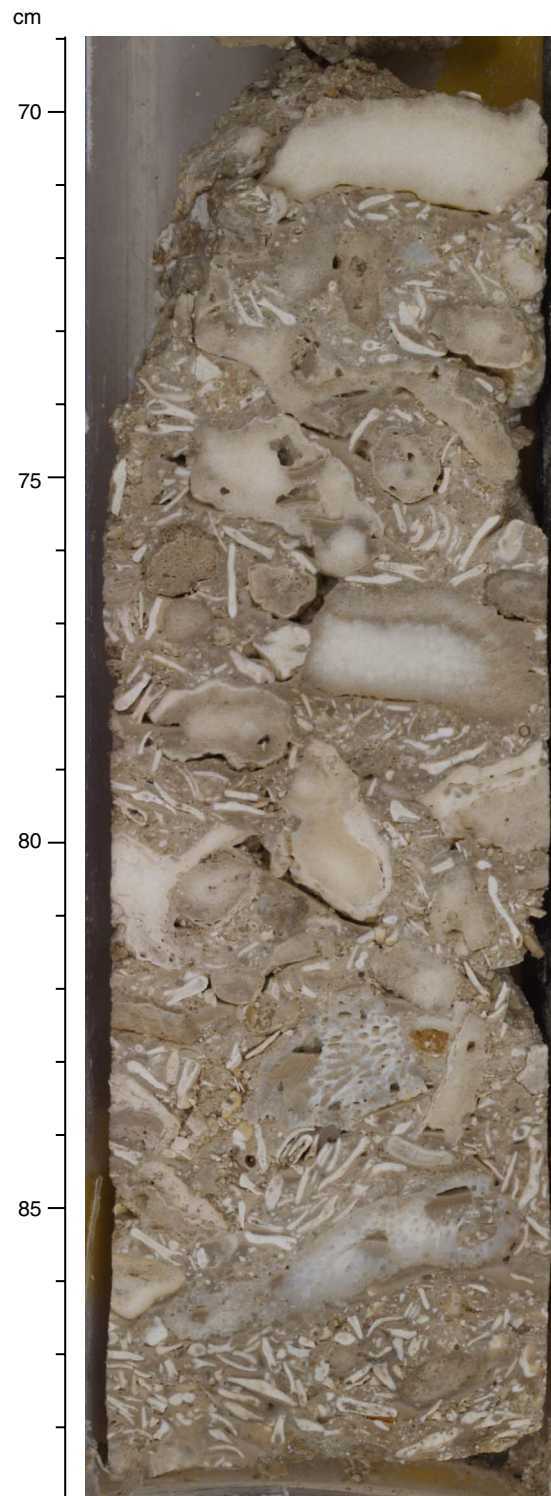


**Figure F16.** Skeletal floatstone rich in *Halimeda* segments and fragments of encrusting *Porites* and robust branching *Pocillopora* (Subunit IIB; interval 310-M0019A-22R-1, 49–70 cm). Upper part of image shows encrusting colonies of *Montipora* and coralline algal crusts.

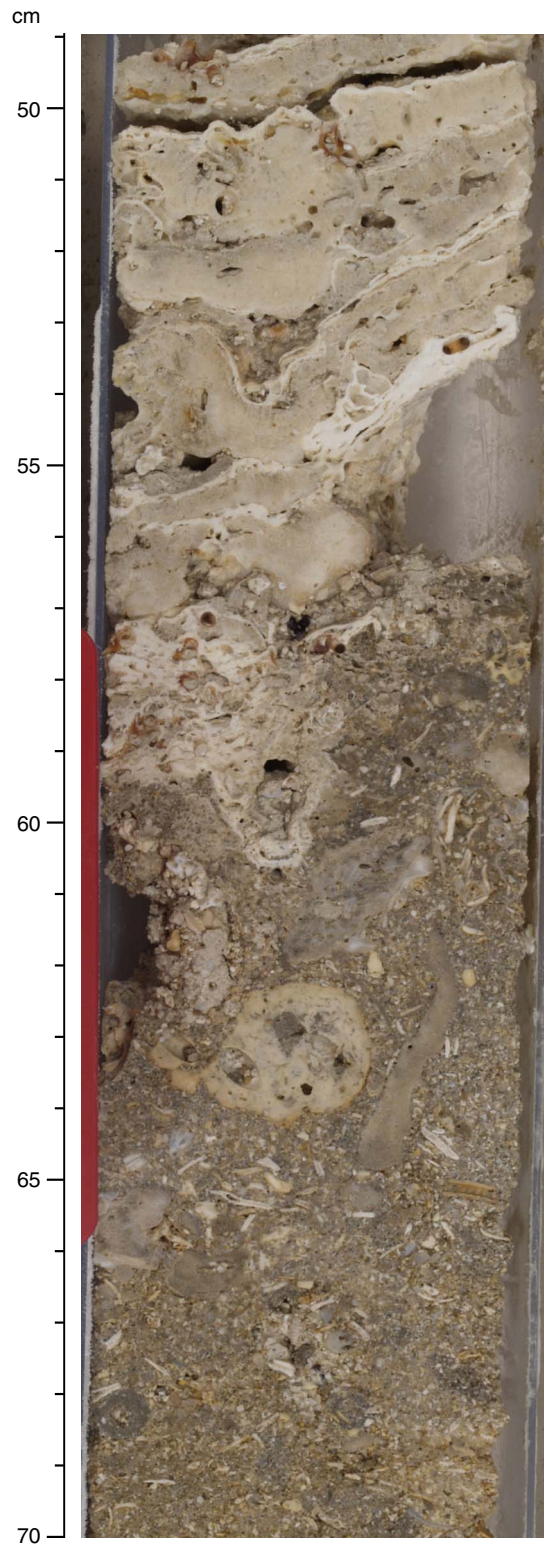


**Figure F17.** Skeletal rudstone with fragments of tabular *Acropora* and encrusting *Porites* and *Halimeda* segments (Subunit IIB; interval 310-M0019A-22R-1, 100–110 cm).

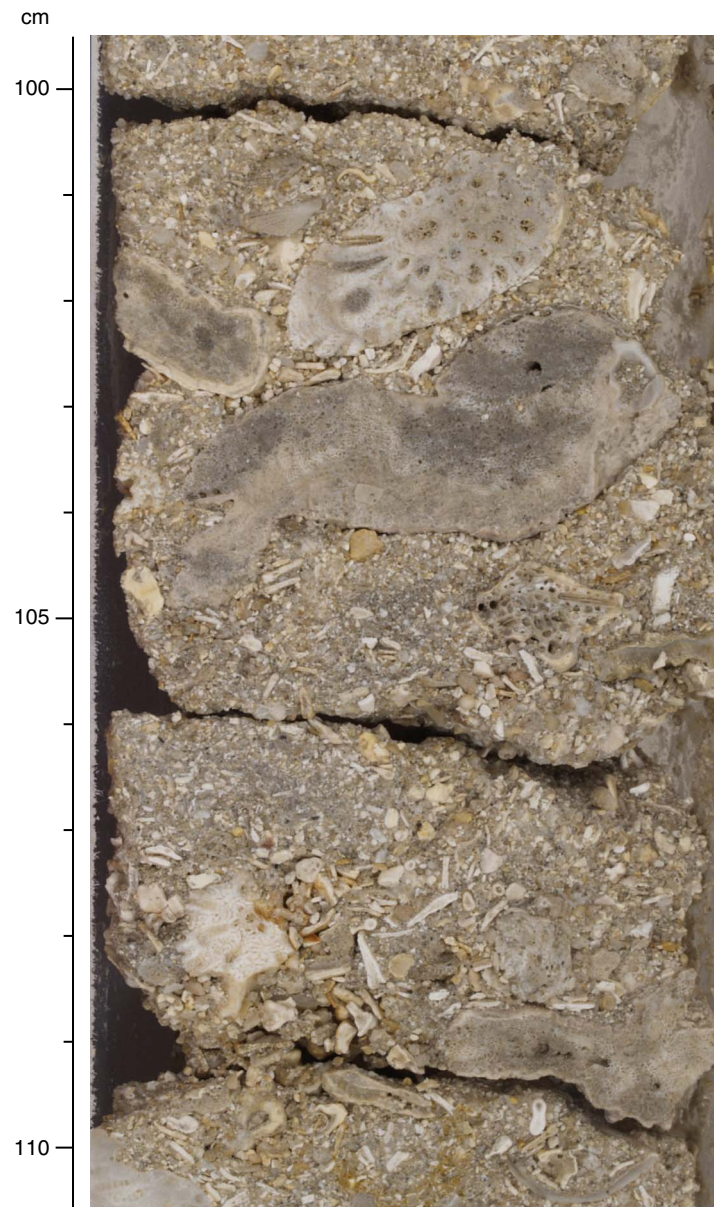


**Figure F18.** Fragments of tabular *Acropora* and robust branching *Pocillopora* associated with skeletal and volcanic coarse sand (Subunit IIB; interval 310-M0019A-27R-1, 38–46 cm).

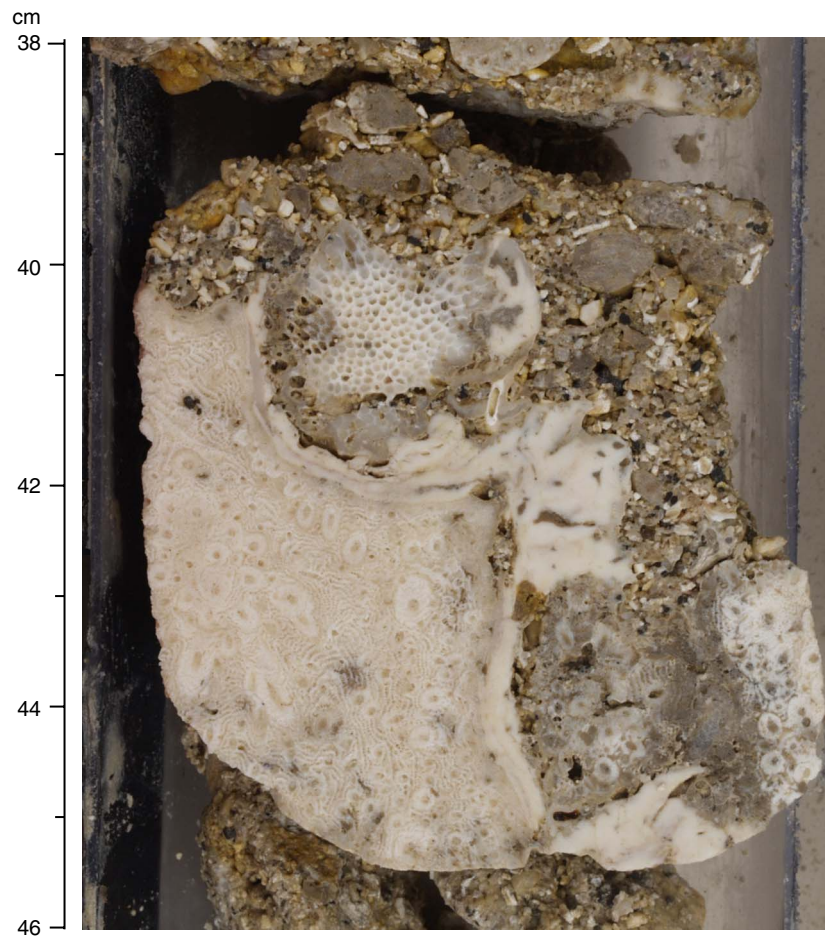


**Figure F19.** Massive colonies of *Porites* encrusted with multiple thin coralline algal crusts (Subunit IIC; interval 310-M0019A-27R-1, 68–84 cm). Primary pore space is filled with coarse skeletal sediment recording volcanic grains.

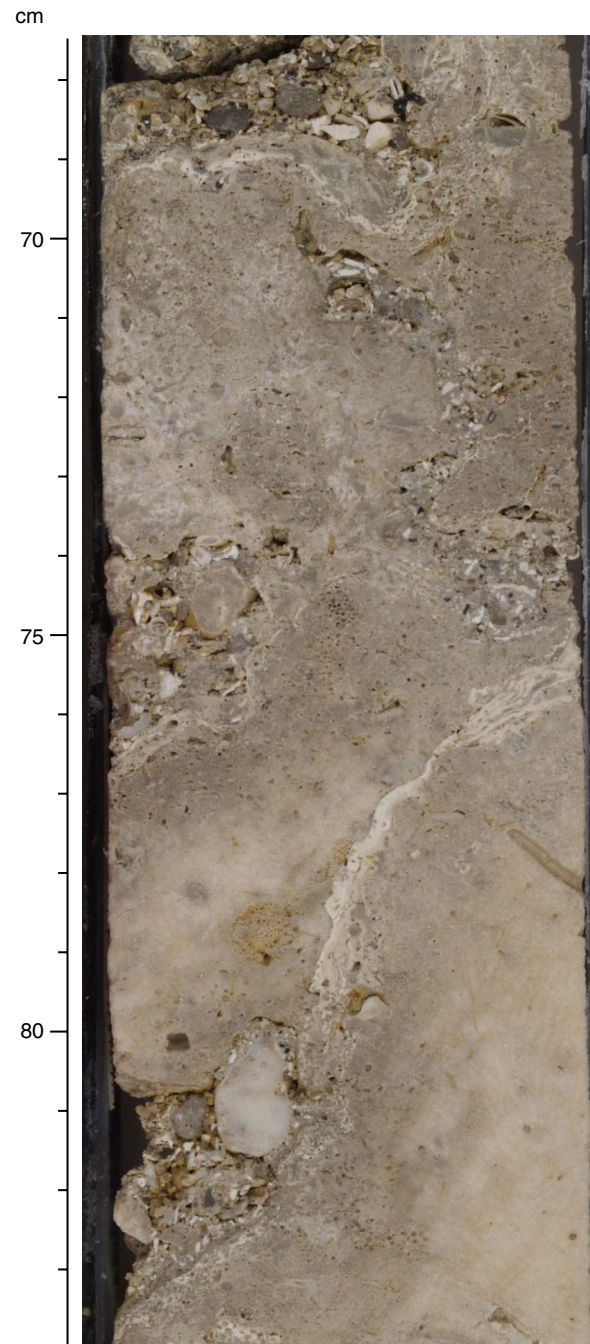


**Figure F20.** Tabular colonies of *Acropora* (Subunit IIC; interval 310-M0019A-32R-1, 45–66 cm). Note volcanic grains in the skeletal grainstone matrix.

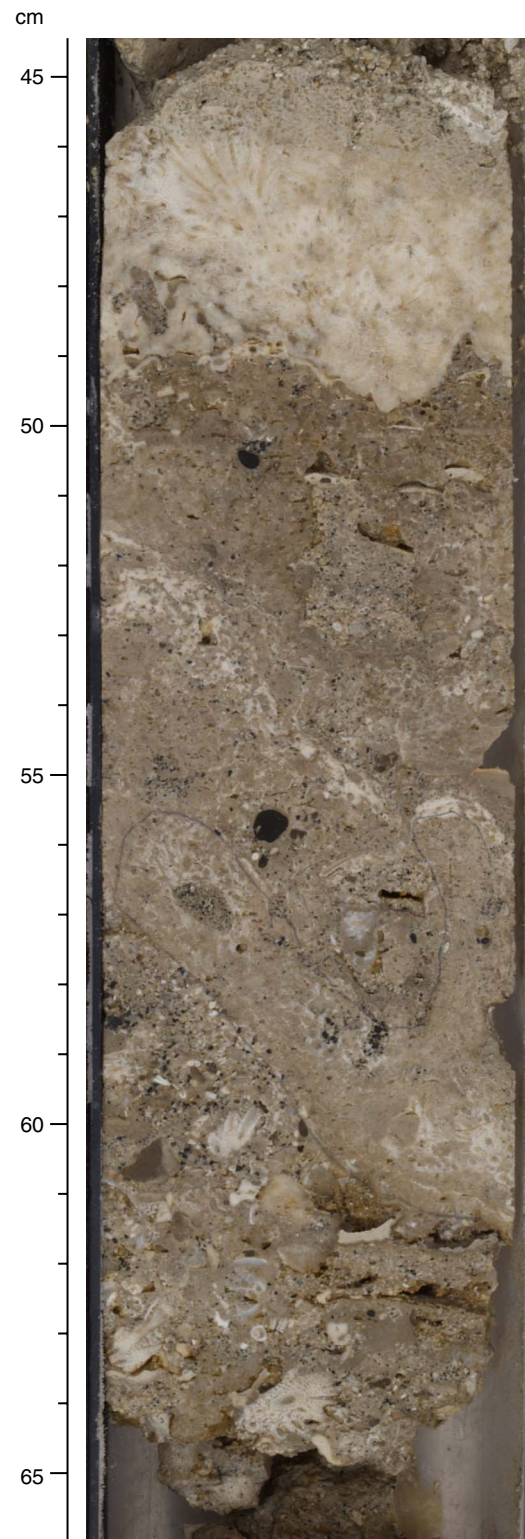


**Figure F21.** Poorly sorted skeletal rudstone with volcanic grains (Subunit IIC; interval 310-M0019A-32R-1, 66–82 cm). Note thin coralline algal crusts between 72 and 76 cm.

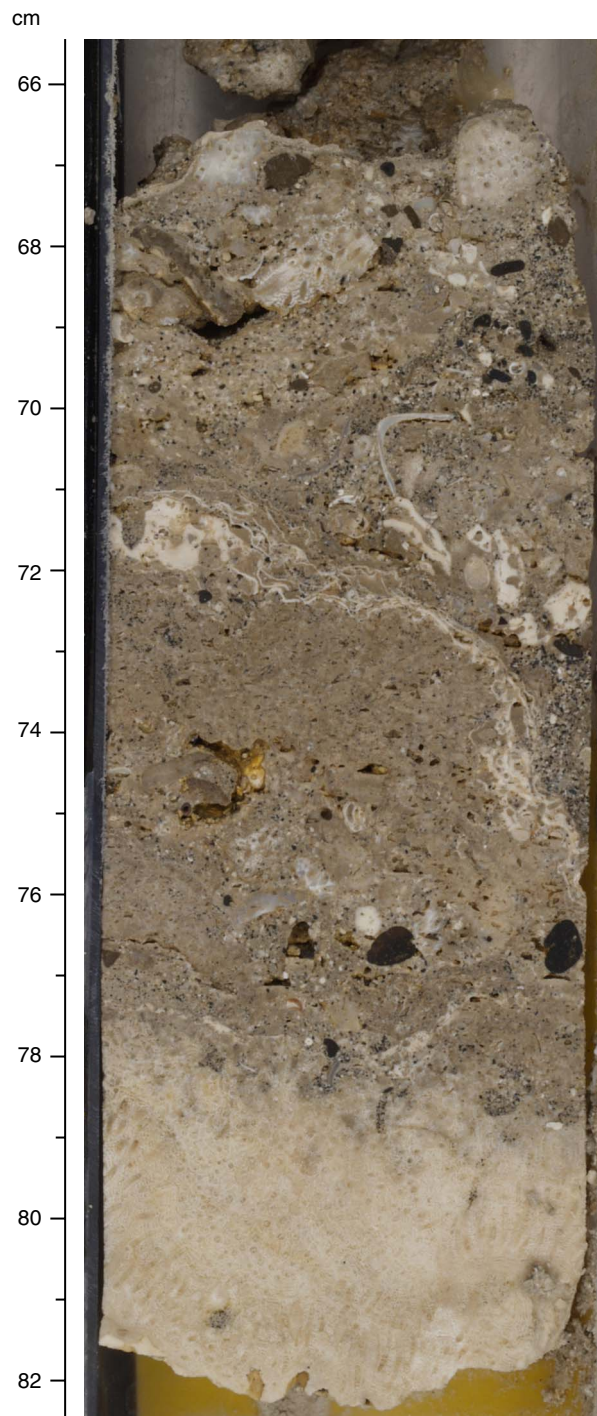


**Figure F22.** Poorly sorted skeletal rudstone with tabular *Acropora* and robust branching *Pocillopora* fragments and rhodoliths (Subunit IIC; interval 310-M0019A-33R-2, 10–34 cm).

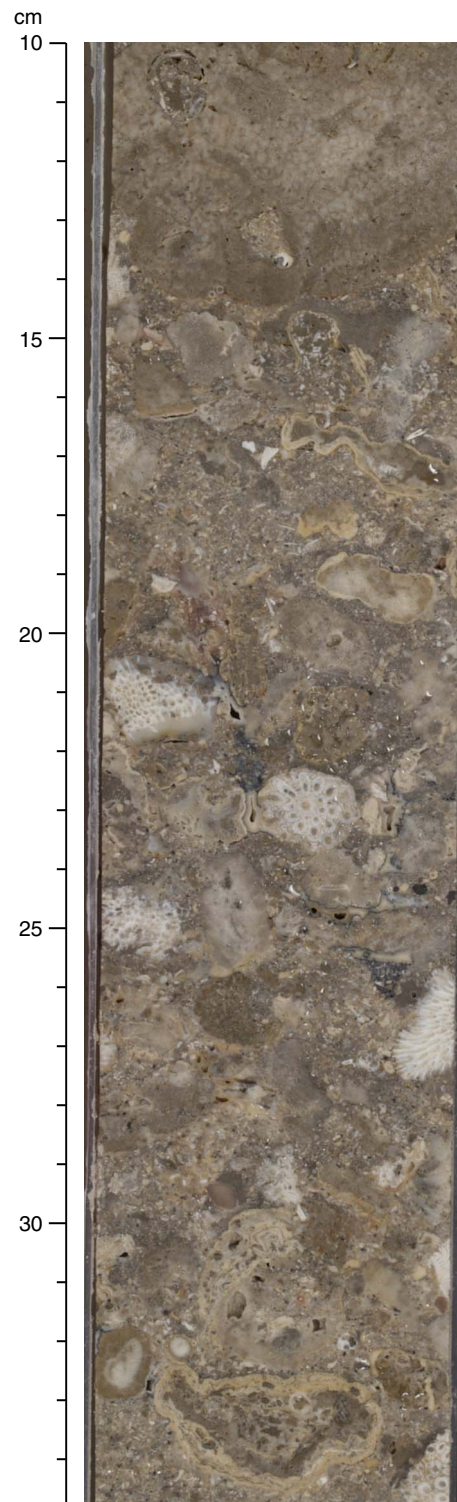
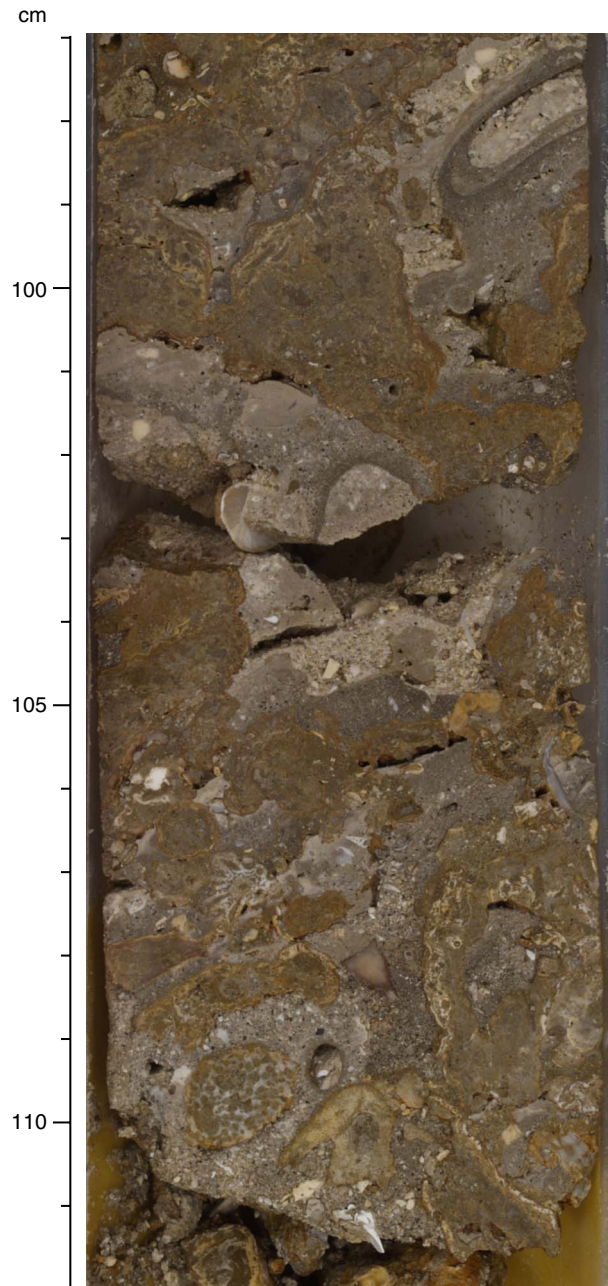
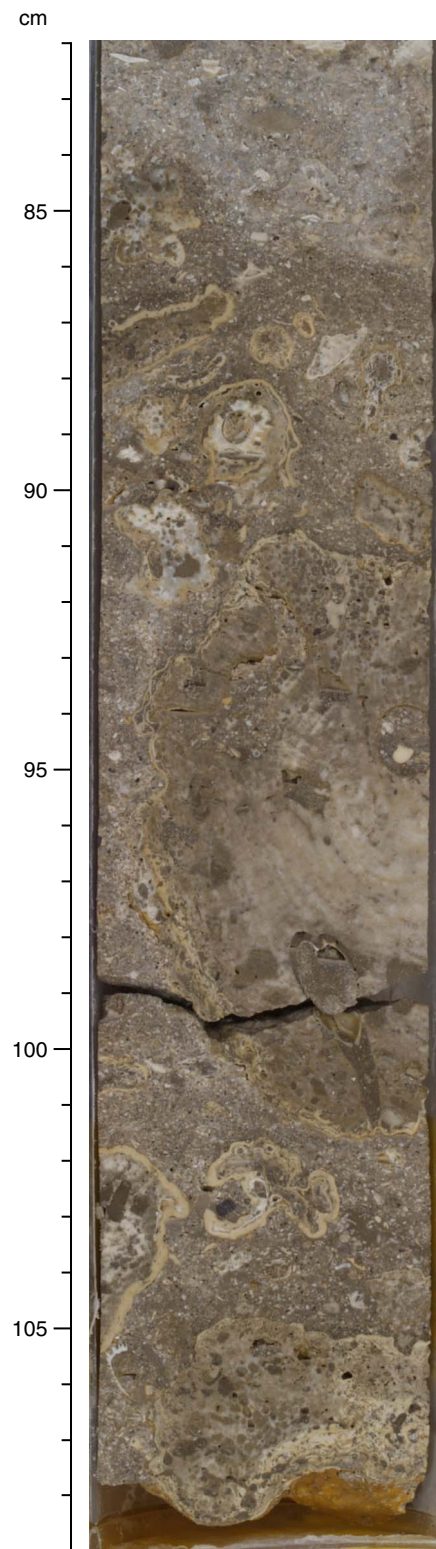


Figure F23. Poorly sorted skeletal rudstone (Subunit IIC; interval 310-M0019A-33R-2, 97–112 cm).



**Figure F24.** Poorly sorted skeletal rudstone with rhodoliths (Subunit IIC; interval 310-M0019A-33R-3, 82–109 cm).



**Figure F25.** Intense bioerosion of encrusting *Montipora* colonies and coralline algal crusts (Unit II; interval 310-M0020A-10R-1, 40–48 cm).

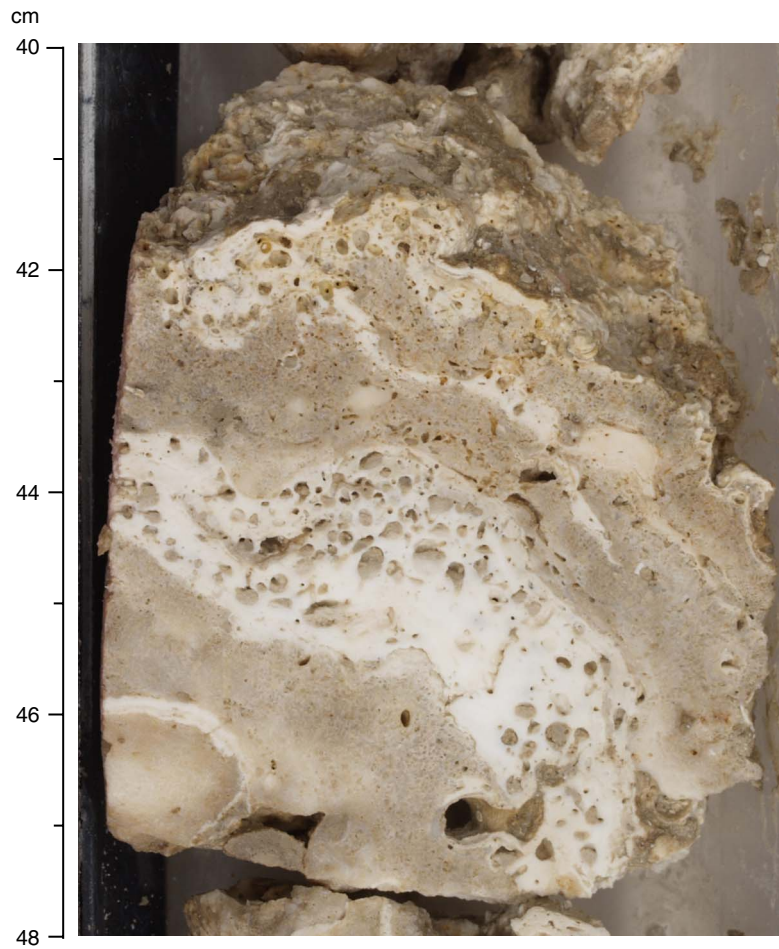


**Figure F26.** Encrusting colonies of *Porites* with multiple encrustations with coralline algae and very thick laminated microbialites (Unit II; interval 310-M0020A-12R-1, 64–80 cm). Note bioerosion of red algal crusts.



**Figure F27.** Thick coralline algal crust on top of a massive *Porites* colony (Unit II; interval 310-M0020A-16R-1, 55–70 cm). Note vermetid gastropod engulfed in coralline algal crust.

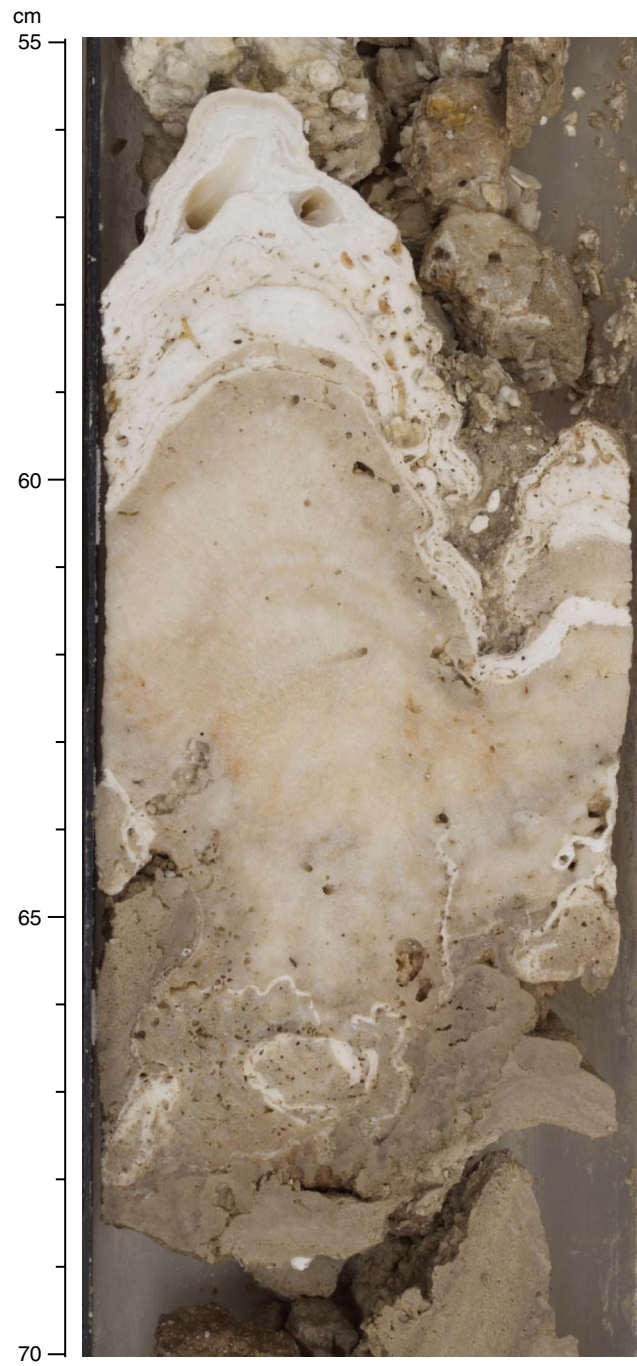


**Figure F28.** Tips of branching *Porites* colonies encrusted with coralline algae (Unit II; interval 310-M0020A-18R-1, 49–58 cm).



**Figure F29.** Encrusting colonies of *Montipora* interlayered with thick encrusting coralline algae engulfing vermetid gastropods (Unit II; interval 310-M0020A-20R-1, 89–101 cm).

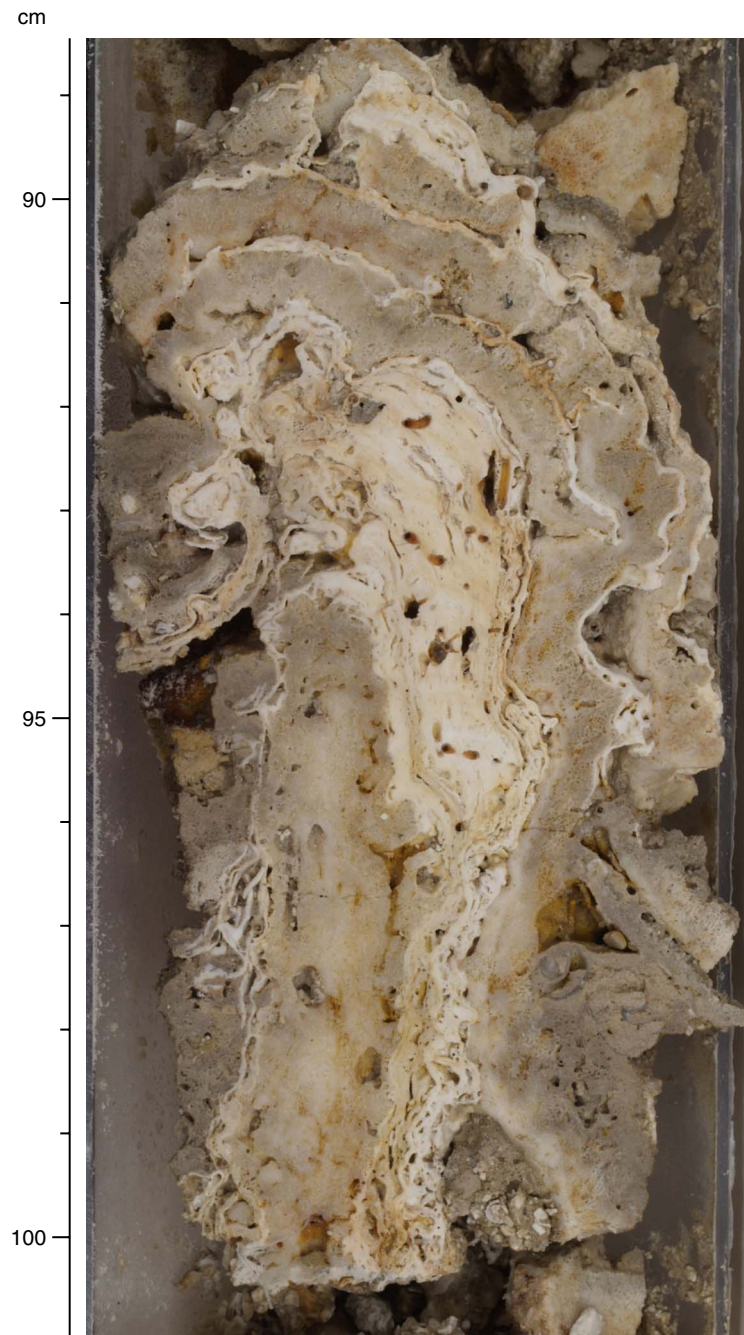


**Figure F30.** Robust branching *Pocillopora* colony (Unit II; interval 310-M0020A-21R-2, 14–23 cm). Lower part of figure is primary vug infilled with microbialite mass.

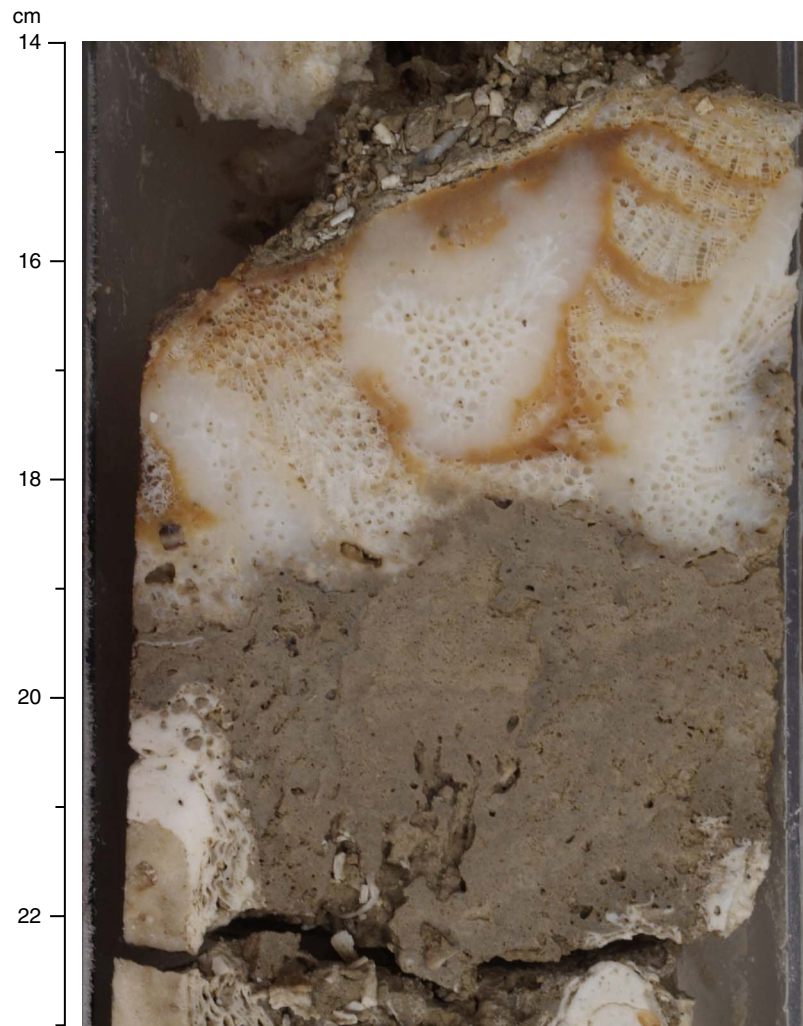


**Figure F31.** Encrustation of coral with coralline algae and laminated microbialites (Unit II; interval 310-M0020A-12R-1, 33–50 cm). Primary pore space is partly filled with *Halimeda*-bearing sediment. Note worm tubes between 39 and 44 cm.

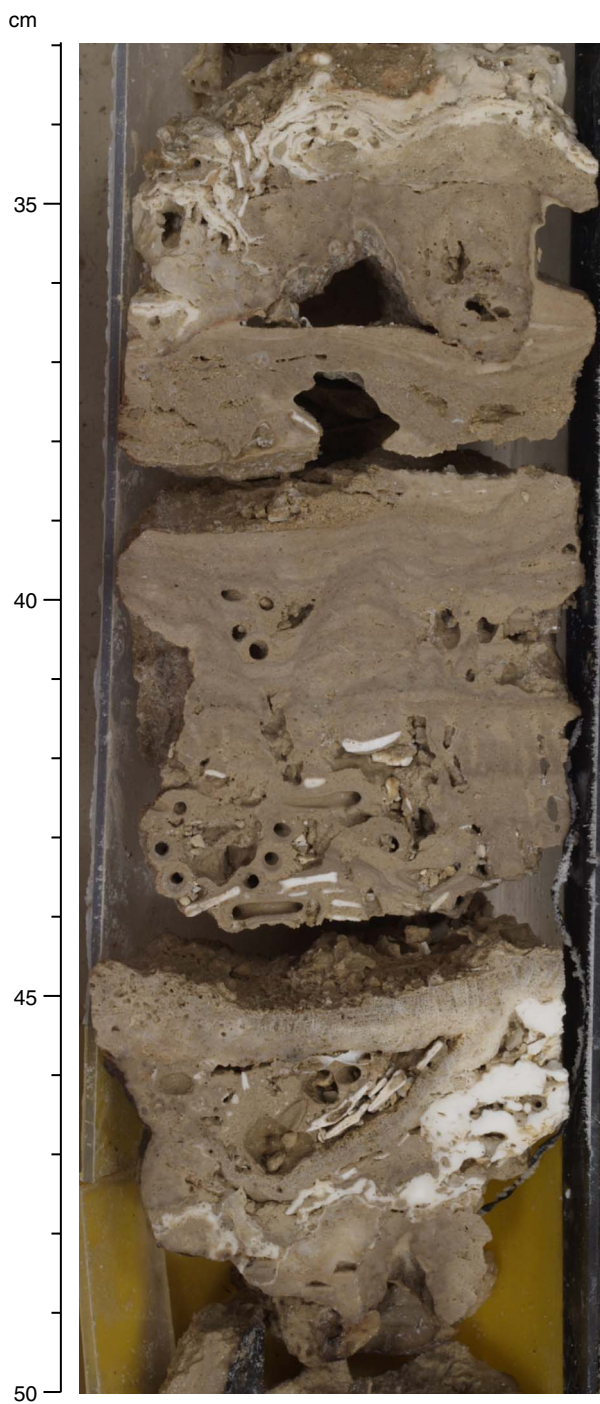


**Figure F32.** Branching colonies of *Porites* encrusted with coralline algae and thick laminated microbialite crusts (Unit II; interval 310-M0020A-18R-2, 1–18 cm).

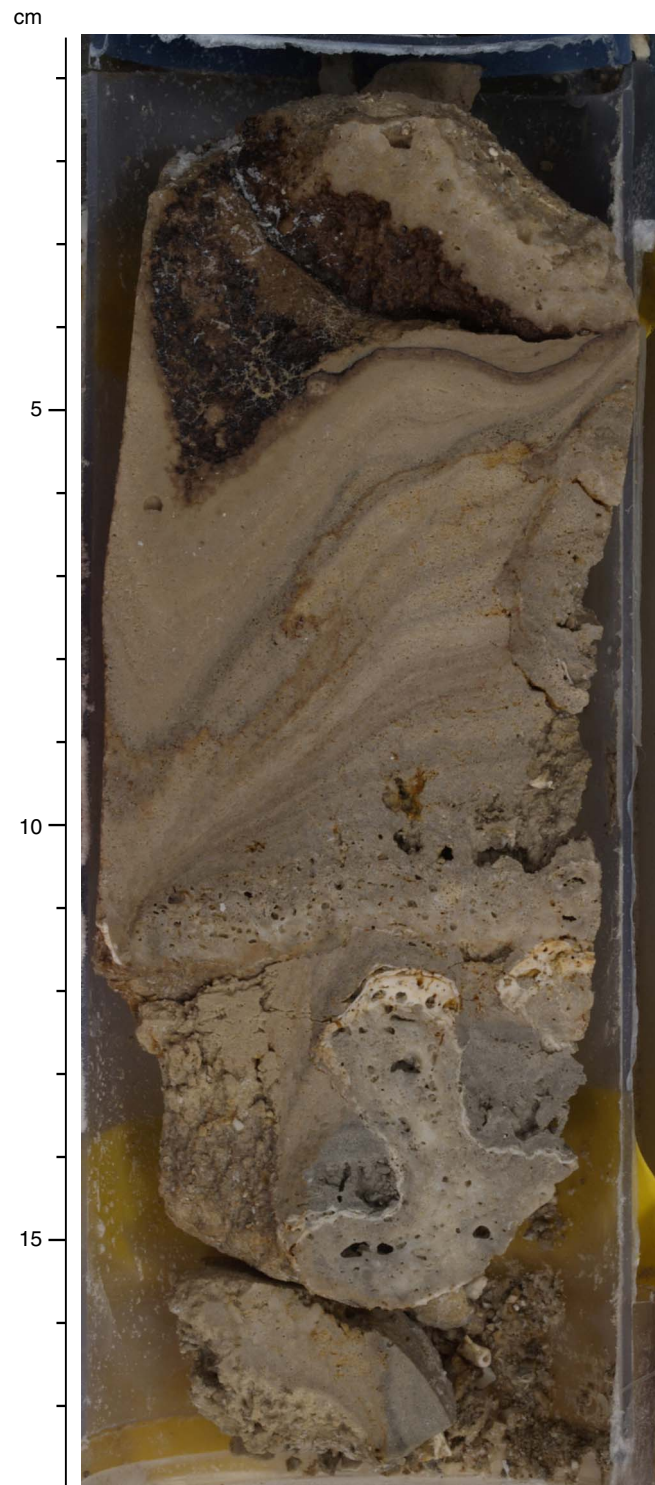


**Figure F33.** Branching *Porites* framework with thick laminated domal microbialite encrustation making up the largest portion of the core (Unit II; interval 310-M0020A-20R-1, 114–149 cm). Note coralline algal crust on tips of branches in lower part of the image.

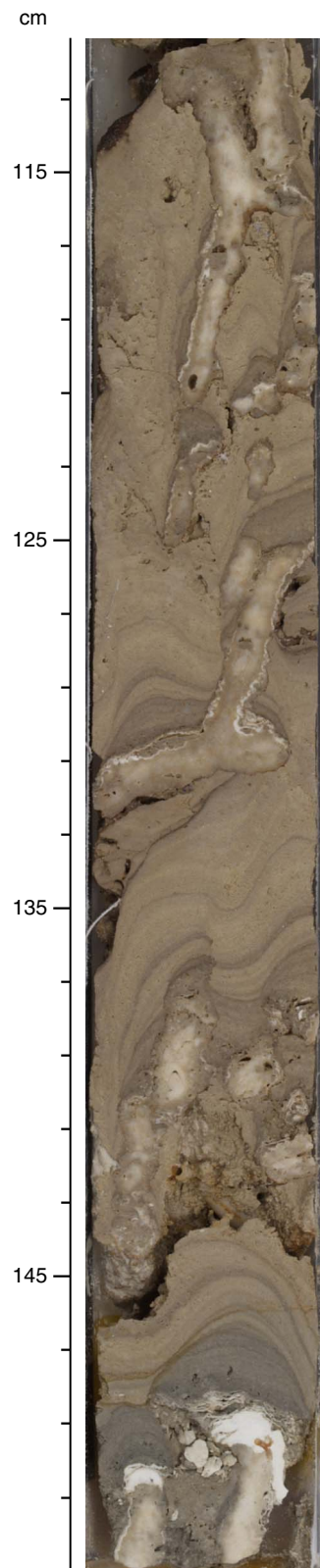


**Figure F34.** Massive colony of *Porites*; primary pore space is infilled with *Halimeda*-rich sediment and laminated microbialite crusts (Unit II; interval 310-M0020A-22R-2, 16–34 cm).

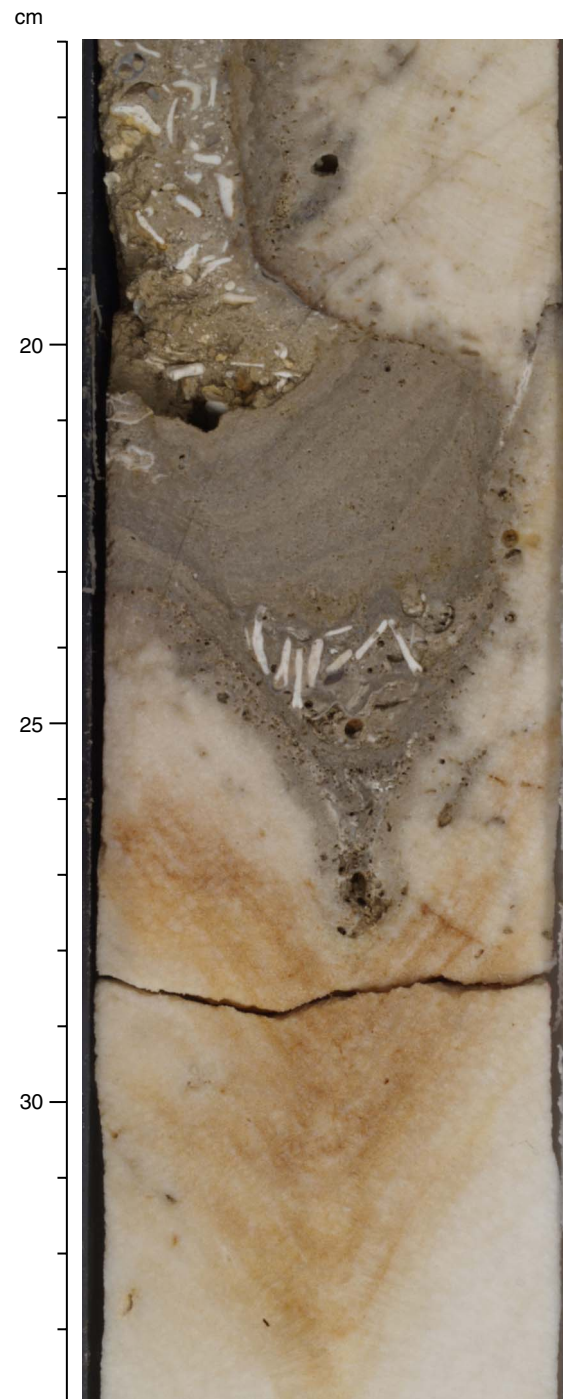


**Figure F35.** *Halimeda* wackestone and rudstone with fragments of branching *Pocillopora* (Unit II; interval 310-M0020A-25R-2, 0–17 cm).

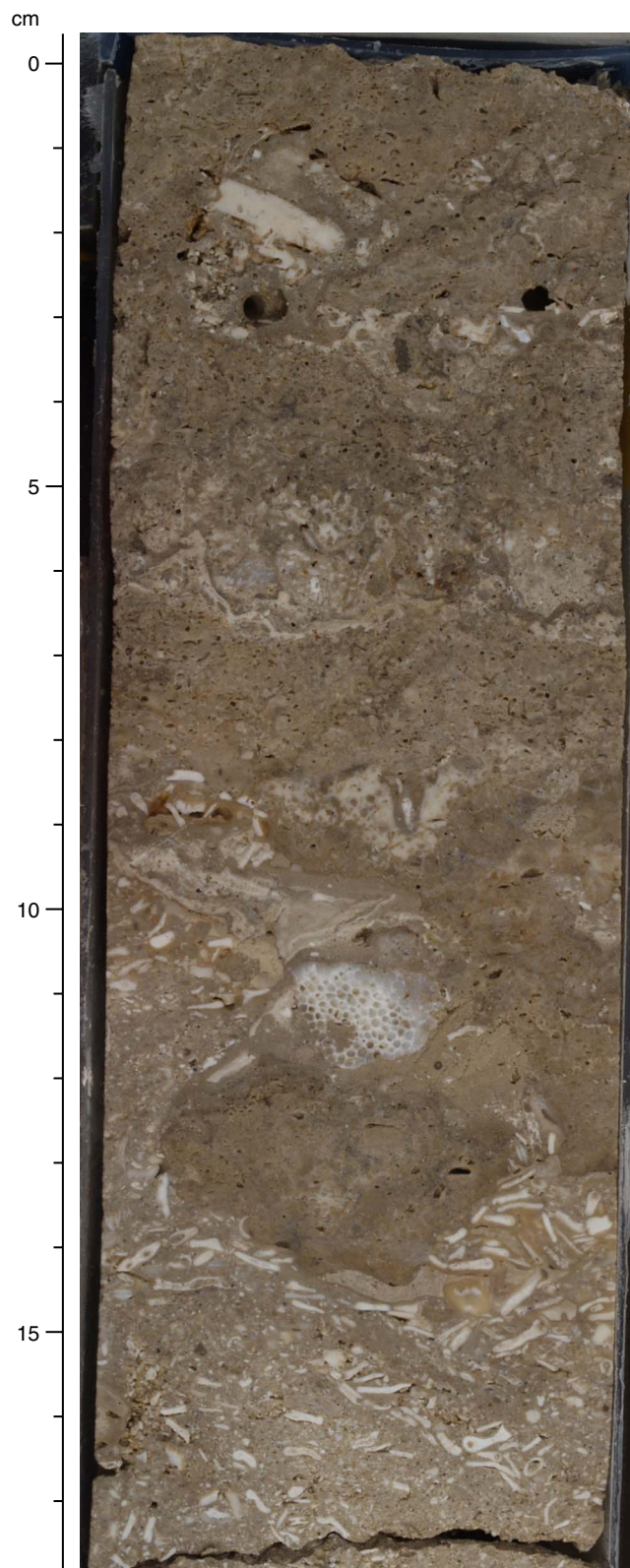


**Figure F36.** Velocity, bulk density, magnetic susceptibility, and porosity as a function of depth in Hole M0019A. Discrete measurements are superimposed (red circles).

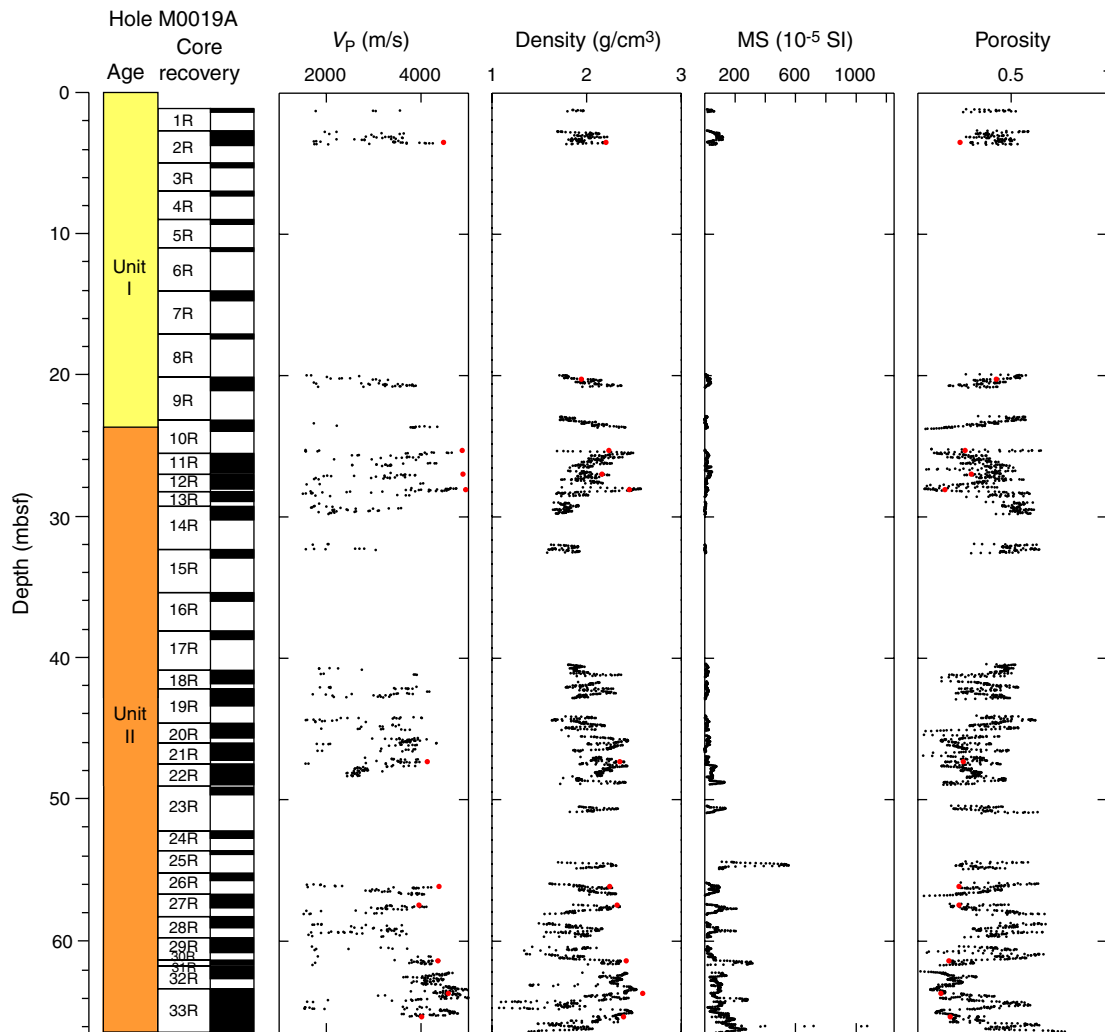


**Figure F37.** Velocity, bulk density, magnetic susceptibility, and porosity as a function of depth in Hole M0020A. Discrete measurements are superimposed (red circles).

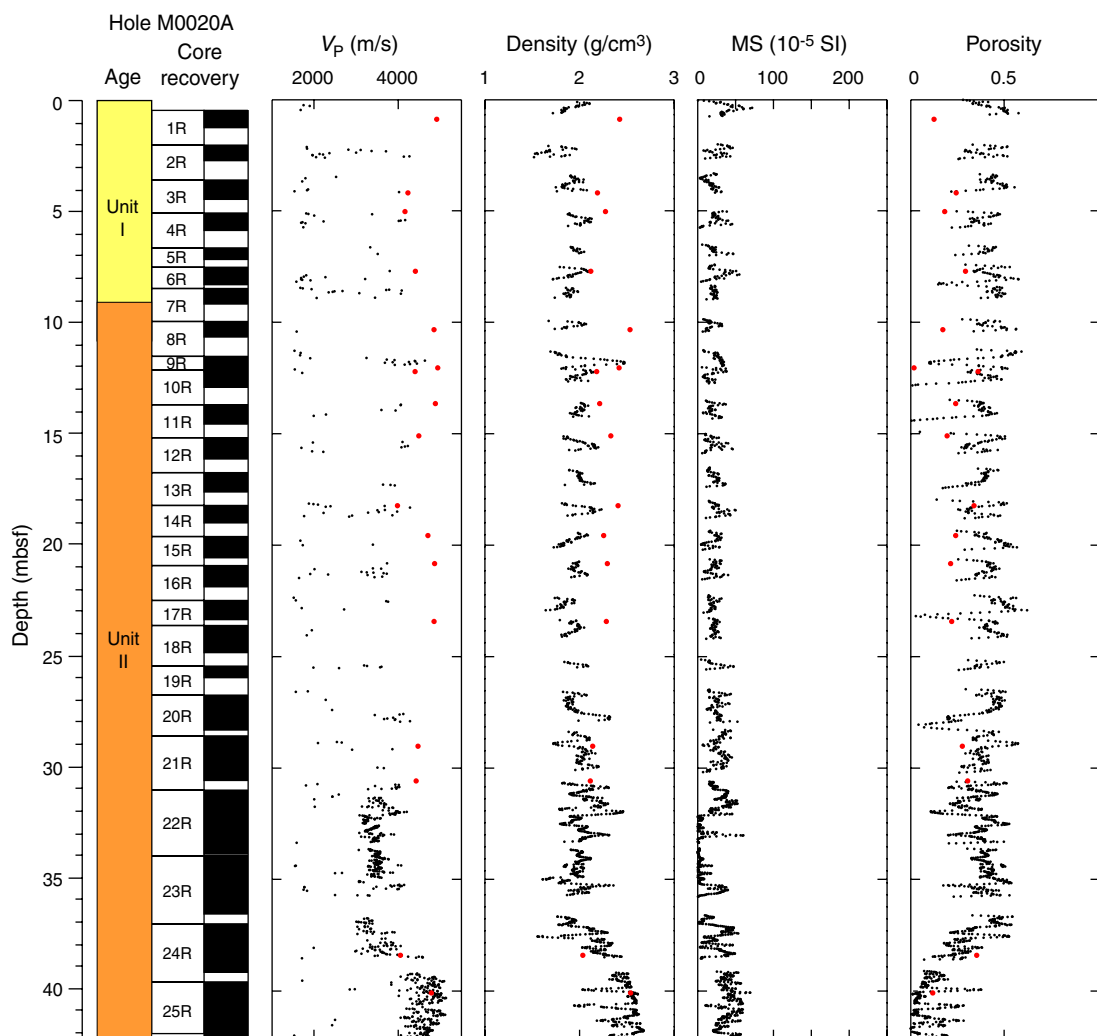


**Figure F38.** Cross plot of porosity with velocity for Site M0019. Solid lines refer to the Wyllie time average equation (red) and Raymer modified time average equation (green) for a matrix velocity of calcite (6530 m/s). Discrete measurements are superimposed (red circles).

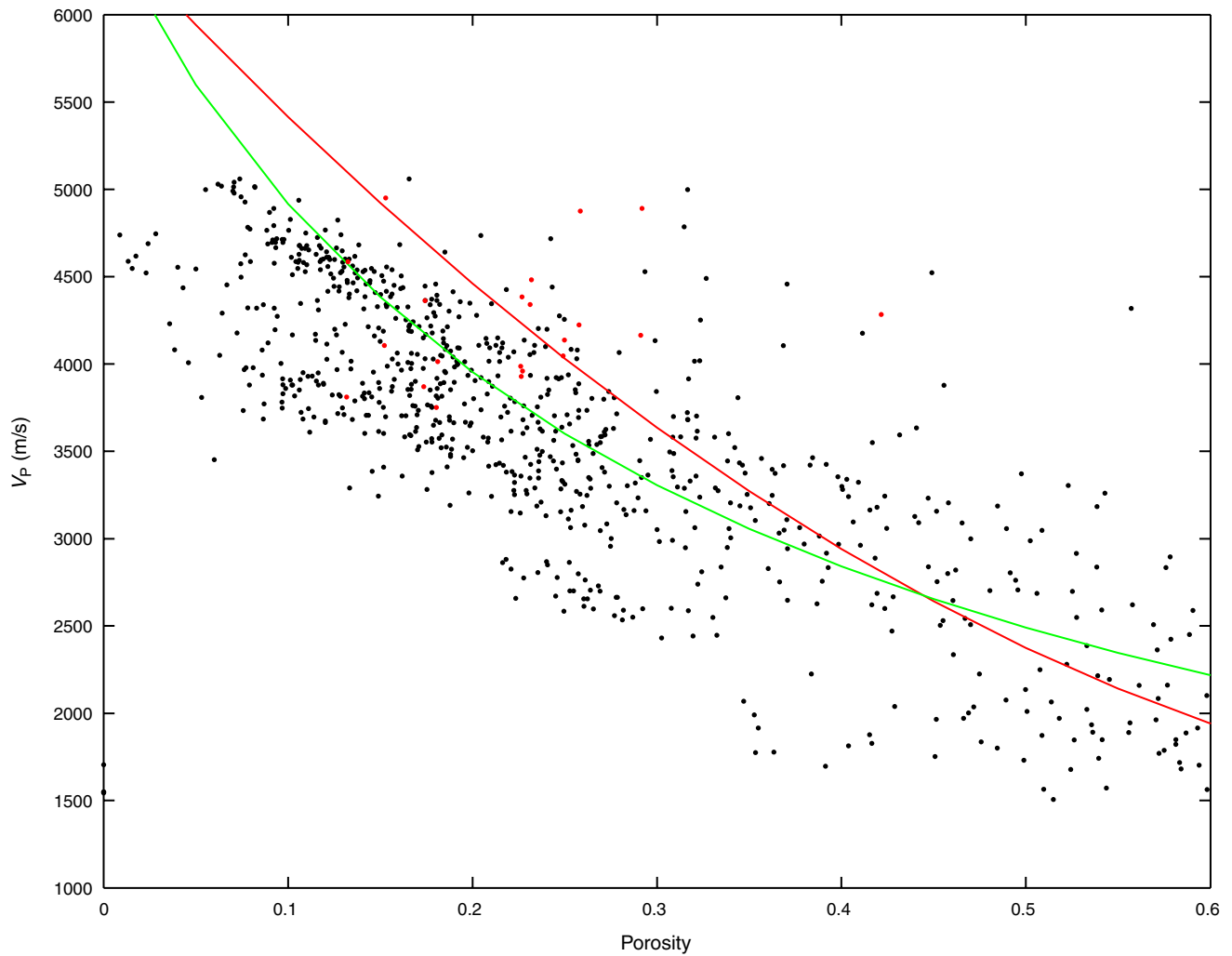


**Figure F39.** Color reflectance ( $L^*$ ) data from Holes M0019A and M0020A. For plotting purposes, Hole M0020 is offset from Hole M0019A by 40  $L^*$  units.

